PROCEEDINGS OF SPIE

SPIEDigitalLibrary.org/conference-proceedings-of-spie

Development of the construction sketch of N-channel MOS-phototransistor with bilateral illumination of channel and operation card of its making

Osadchuk, Alexander, Osadchuk, Vladimir, Zhahlovska, Olena, Luganskaya, Saule, Kociubiński, Andrzej

Alexander V. Osadchuk, Vladimir S. Osadchuk, Olena M. Zhahlovska, Saule Luganskaya, Andrzej Kociubiński, "Development of the construction sketch of N-channel MOS-phototransistor with bilateral illumination of channel and operation card of its making," Proc. SPIE 10808, Photonics Applications in Astronomy, Communications, Industry, and High-Energy Physics Experiments 2018, 108080R (1 October 2018); doi: 10.1117/12.2501552

Event: Photonics Applications in Astronomy, Communications, Industry, and High-Energy Physics Experiments 2018, 2018, Wilga, Poland

SPIE.

Downloaded From: https://www.spiedigitallibrary.org/conference-proceedings-of-spie on 13 Nov 2021 Terms of Use: https://www.spiedigitallibrary.org/terms-of-use

DEVELOPMENT OF THE CONSTRUCTION SKETCH OF N-CHANNEL MOS - PHOTOTRANSISTOR WITH BILATERAL ILLUMINATION OF CHANNEL AND OPERATION CARD OF ITS MAKING

[1]Alexander V. OSADCHUK, [1]Vladimir S. OSADCHUK, [1]Olena M. ZHAHLOVSKA, [2]Saule LUGANSKAYA, [3]Andrzej KOCIUBIŃSKI
[1]Vinnytsia National Technical University, Khmelnytsky highway 95, 21021Vinnytsia, Ukraine
[2]Caspian University, Almaty, Kazakhstan
[3]Lublin University of Technology, Lublin, Poland

Abstract. In the article the physical mechanism of optical radiation co-operation with semiconductor devices, technological route of making of MOS - phototransistor with bilateral illumination of channel has been considered. Also the optical transducer with frequency output based on the structure of the bipolar-field transistors with negative resistance and MOSFET with bilateral illumination of channel that is a photosensitive element has been considered. A mathematical model of the radiomeasuring optical transducer has been developed.

Keywords: frequency optical transducer, phototransistor, negative resistance.

1. INTRODUCTION

On this stage of scientific and technical progress there is intensive development of semiconductor devices for optical radiation power measuring. Due to the use of new microelectronics technologies provided making of microelectronic scopes, that have a high sensitiveness to the measuring parameter and insensitivity to other external factors, and also characterized by a small energy consumption and complete informing compatibility with microprocessor facilities of information treatment [1-5].

The frequency method of optical radiation power transformation has the above-mentioned advantages. And for realization of this method it is necessary to analyse the physical mechanism of optical radiation co-operation with semiconductor devices [6]. Therefore this paper is sanctified to the analysis of the physical phenomena in semiconductors and semiconductor devices, that allowed to ground legitimacy of its photoreactive properties application for creation of radiomeasuring devices on the basis of optical transducers with a frequency output [7].

Currently microelectronic physical quantities transducers are widely used in different applications, and their advantages over traditional due primarily to using them as sensitive elements of semiconductor materials, methods of group formation and processing them into measuring circuits' amplification and signal processing techniques of microelectronic technology [8].

2. CONSTRUCTION OF MOS - PHOTOTRANSISTOR WITH BILATERAL ILLUMINATION OF CHANNEL

The developed mathematical model of optical transducer must take into account effects that arise up at interaction of optical radiation with semiconductor devices. As a photosensitive element in a similar optical transducer is MOS FET with bilateral illumination of channel.

The MOS-phototransistors with a semilucent electrode through that a gate area is illuminated are known. It is also known, that the gate electrode of thin-film MOSFET can be opaque, and illumination carry out through substrate. A not high photo-response and complicated technology behave to the lacks of such devices [9-10].

In the known phototransistor on the basis of MOS - structure that contains the semiconductor substrate, one of surfaces of that is radiation-sensitive, with the areas of drain, source and channel, on that the dielectric layer and gate electrode are formed. The substrate's surface without dielectric is radiation-sensitive and has slots above the area of channel [11].

In order to extend the functional possibilities, namely: increase of phototransistor's sensitiveness to the radiation, in the offered construction of MOSFET, that contains substrate from $p-Si$ ($N_D = 10^{17}\,cm^{-3}$), with a semilucent

Photonics Applications in Astronomy, Communications, Industry, and High-Energy Physics Experiments 2018, edited by Ryszard S. Romaniuk, Maciej Linczuk, Proc. of SPIE Vol. 10808, 108080R
© 2018 SPIE · CCC code: 0277-786X/18/$18 · doi: 10.1117/12.2501552

Downloaded From: https://www.spiedigitallibrary.org/conference-proceedings-of-spie on 13 Nov 2021
Terms of Use: https://www.spiedigitallibrary.org/terms-of-use

gate electrode of *Al*, through that a gate area is illuminated, from the reverse of substrat under the area of channel deep slots are executed. Sectional plane each of them satisfies to correlation $A < S/n$, where S is an area of channel, n is a number of slots. Thus a depth of slots must be such, that a condition $\alpha d \rightarrow 1$ was executed, where α is an absorption coefficient, d is a thickness of wafer between a slot's bottom and gate dielectric (fig. 1). Thus, illumination occurred through substrate, and through a gate.

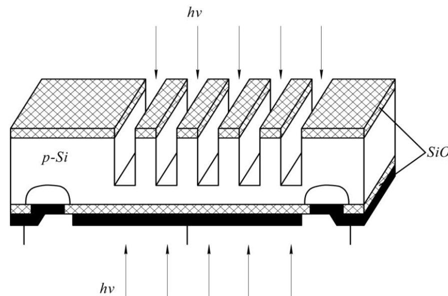

Fig. 1. Construction of MOS - phototransistor with bilateral illumination of channel [11].

This MOS phototransistor works thus [11]. The voltage is applied between the area of source and drain thus, that drain junction was displaced in reverse direction, and sourse junction had a zero or small positive bias. The voltage between a gate and substrate must equal or be over threshold. Thus voltage of drain-sourse p-n junction and of backward-biased p-n junction drain-substrate and of sourse-substrate p-n junction must be considerably less than, than bias between the area of gate and substrate. A signal appears on the device output as a result of illumination simultaneously of all slots by a radiation with a wave-length, that corresponded an internal photoeffect in a semiconductor. If only one of slots is illuminated, then output signal will be far less the maximal level and can be accepted as a logical zero. At the complete darkening of all slots an output signal also is very small and corresponded a zero level.

For providing of sufficient phototransistor's sensitiveness to the radiation it is necessary to ensure, that at this amount of slots their sectional area was maximal and, that they as possible nearer fit closely to the upper bound of the induced channel by the lower butt-end. In an order to prevent light dispersion on slots, minimum diameter of every slot and minimum distance between nearby slots must be not less than on an order must exceed the wave-length of radiation.

3. SCALE CONSTRUCTION SKETCH OF N - CHANNEL MOS - PHOTOTRANSISTOR WITH BILATERAL ILLUMINATION OF CHANNEL

Scale construction sketch of n - channel MOS - phototransistor with p – substrate and n^+ – gate is shown in Figure 2.

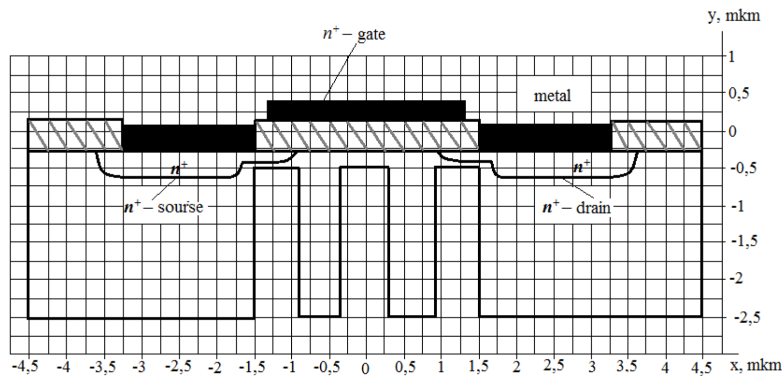

Fig.2. Scale construction sketch of n - channel MOS - phototransistor with bilateral illumination of channel.

MOSFETs are widely used in composition of integral microcircuits (IMC), as they allow to obtain the concordance of circuits with each other and realize boolean functions. The first in an industrial production were p – MOS circuits. Making of n – MOS circuits is complicated by an origin on the surface of *p - Si* at the thermal oxidizing of inverse n – layer, which electrically connects elements of IMC. Due to the improvement of technology for today in a production prevail n - channel IMC, that have a greater fast-acting due to high mobility of electrons. Next to IMC, that

Downloaded From: https://www.spiedigitallibrary.org/conference-proceedings-of-spie on 13 Nov 2021
Terms of Use: https://www.spiedigitallibrary.org/terms-of-use

contain transistors with the channels of one type, the complementary microcircuits CMOS, that contain transistors with the channels of opposite types, are also made.

IMC on the basis of MOSFETs are made by planar technology and epiplanar technology. Due to more simple construction of MOS-phototransistor and self-isolation of elements the common amount of technological operations diminishes as compared to bipolar technology. It increases the efficiency of suitable IMC and diminishes their cost.

Technological route of making of MOS - phototransistor with bilateral illumination of channel consists of such operations [12]:

1. Choice of substrate: *p* – type silicon, contains boron as dopant, resistivity 10 Ω•cm ($N=10^{15} см^{-3}$), crystal orientation (100).
2. Oxidation: T=950°C, oxidizing atmosphere O_2+H_2O.
3. Photolithography 1. Opening gaps in photoresist surface for slots:
   - Local etching;. Slots formation;
   - Photoresist removal: solution caro, peroxymonosulphuric acid, (in solution $H_2SO_4+ H_2O_2$);
   - chemical treatment: solution caro (in solution $H_2SO_4+ H_2O_2$);
   - Sensitive film coating;
   - chemical treatment of contact hole: solution «caro»;
   - oxidation: T=950°C, oxidizing atmosphere O_2+H_2O;
   - etching-out SiO_2: front end etchant;
   - chemical treatment: solution «caro» (in solution $H_2SO_4+ H_2O_2$);
   - oxidation: T=950°C, oxidizing atmosphere O_2+H_2O;
   - chemical treatment: solution «caro» (in solution $H_2SO_4+ H_2O_2$);
   - oxidation: T=950°C, oxidizing atmosphere O_2+H_2O.
4. Photolithography 2. Mask creation for ion-implantation doping of areas n^+ – drain/sourse:
   - ion-implantation doping by phosphorus, formation of areas n^+ – drain/sourse: $E=60keV$, $D=700mkKl/cm^2$;
   - Photoresist removal: plasma chemical etching + solution «caro»;
   - chemical treatment: solution «caro» (in solution $H_2SO_4+ H_2O_2$).
5. Photolithography 3. Mask creation for contact hole etching to polysilicon of areas n^+ – drain/sourse:
   - phosphoric silicate glass etching: front end etchant;
   - reactive ion etching of phosphoric silicate glass;
   - photoresist removal: «caro» (в розчині $H_2SO_4+ H_2O_2$);
   - chemical treatment: solution «caro» (in solution $H_2SO_4+ H_2O_2$);
   - contact hole treatment;
   - deposition of metal: Al+1%Si.
6. Photolithography 4. Creation of metal interconnection:
   - reactive ion etching of metal;
   - Photoresist removal: plasma chemical etching;
   - hemical treatment;
   - deposition of SiO_2: T=200°C.
7. Photolithography 5. Creation of passivation contact hole:
   - reactive ion etching;
   - Photoresist removal: plasma chemical etching;
   - chemical treatment;
   - metal burn-in: T=400°C;
   - coating of insulating layer.

Technological routing is executed as a table 1.

Table 1 – Technological routing of n - channel MOS - phototransistor with bilateral illumination of channel making

№	Technological operations	production mode	addition
1	Oxidation	T=950°C, oxidizing atmosphere O_2+H_2O	$d_x = 0.036\mu m$
2	Photolithography 1. Opening gaps in photoresist surface for slots		

Downloaded From: https://www.spiedigitallibrary.org/conference-proceedings-of-spie on 13 Nov 2021
Terms of Use: https://www.spiedigitallibrary.org/terms-of-use

3	Local etching for slots formation		$a = 0.6 \cdot 10^{-6}\, m,\ b = 2 \cdot 10^{-6}\, m$
4	Photoresist removal	solution «caro» (H_2SO_4+ H_2O_2)	
5	Chemical treatment	solution «caro»	
6	Etching of SiO_2	front end etchant	
7	Sensitive film coating	BaF_2 or MgF_2	
8	Oxidation (oxide formation)	T=950°C, oxidizing atmosphere O_2+H_2O	$d_x = 0.85 \mu m$
9	Etching of SiO_2	front end etchant	
10	Chemical treatment	solution «caro»	
11	Oxidation	T=950°C, oxidizing atmosphere O_2+H_2O	$d_x = 0.05 \mu m$
12	Chemical treatment	solution «caro»	
13	Oxidation	T=950°C, oxidizing atmosphere O_2+H_2O	$d_x = 0.036 \mu m$
14	Chemical treatment	solution «caro»	
15	Photolithography 2. Mask creation for ion-implantation doping of areas n^+ – drain/sourse		
16	Ion-implantation doping by phosphorus. Formation of areas n^+ – drain/sourse	$E = 60 keV$ $D = 700 \mu Kl / cm^2$	$x_{ds} = 0.3 \mu m$
17	Photoresist removal	plasma chemical etching + solution «caro»	
18	Chemical treatment	solution «caro»	
19	Photolithography 3. Mask creation for contact hole etching to polysilicon of areas n^+ – drain/sourse		
20	Etching of phosphoric silicate glass	front end etchant	$Min\, d_{x(зал)} = 0.50 \mu m$ (on SiO_2)
21	reactive ion etching of phosphoric silicate glass		$Min\, d_{x(зал)} = 0.01 \mu m$ (on SiO_2)
22	Photoresist removal	solution «caro»	
23	Chemical treatment	solution «caro»	
24	Chemical treatment of contact hole		
25	Deposition of metal	Al+1%Si	$d_x = 1.0 \mu m$
26	Photolithography 4. Creation of metal interconnection		
27	reactive ion etching of metal		
28	Photoresist removal	plasma chemical etching	
29	Chemical treatment		
30	deposition of SiO_2	T=200°C	$d_x = 0.20 \mu m$
31	Photolithography 5. Creation of passivation contact hole		
32	reactive ion etching		
33	Photoresist removal	plasma chemical etching	
34	Chemical treatment		
35	metal burn-in	T=400°C	
36	coating of insulating layer		

Downloaded From: https://www.spiedigitallibrary.org/conference-proceedings-of-spie on 13 Nov 2021
Terms of Use: https://www.spiedigitallibrary.org/terms-of-use

The technological route of making of n-MOS phototransistor with bilateral illumination of channel is presented as a flowsheet that shows the cross-section of structure on the key stages of making (fig. 3 – fig. 11).

For development of complete route of MOS-pfototransistor with bilateral illumination of channel making with certain parameters it is necessary to expect threshold tension and suballoying dose, to compensate this tension. It is also necessary to expect ions energies and irradiation dose that necessary for creation of p - n junction.

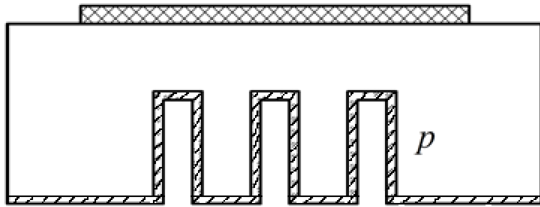

Fig. 3. Cross-section draft of MOSFET structure (operations of technological routing № 1 – 8).

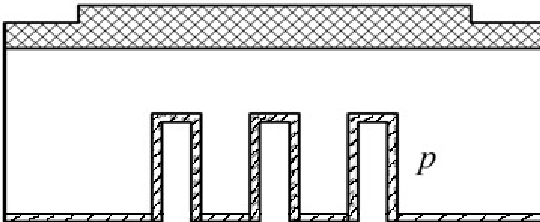

Fig. 4. Cross-section draft of MOSFET structure (operations of technological routing №9 – 13).

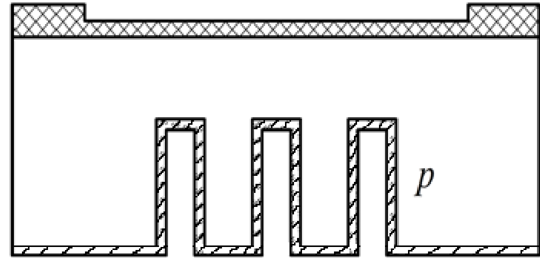

Fig. 5. Cross-section draft of MOSFET structure (operations of technological routing № 14 – 15).

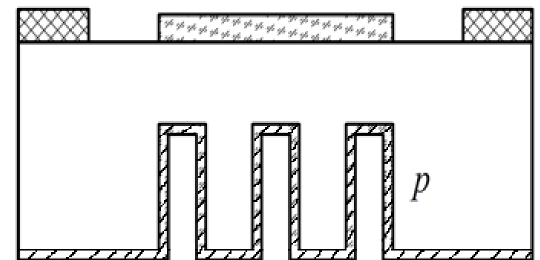

Fig. 6. Cross-section draft of MOSFET structure (operations of technological routing № 16 – 17).

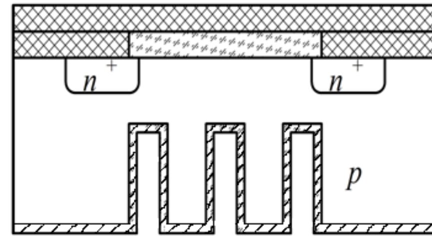

Fig. 8. Cross-section draft of MOSFET structure (operations of technological routing № 21 – 23).

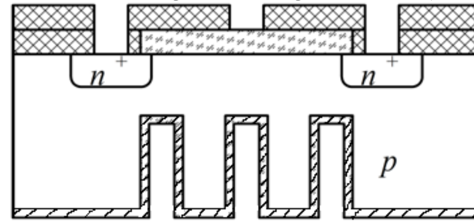

Fig. 9. Cross-section draft of MOSFET structure (operations of technological routing № 24 – 26).

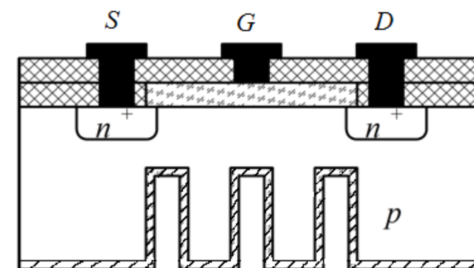

Fig. 10. Cross-section draft of MOSFET structure (operations of technological routing № 27 – 33).

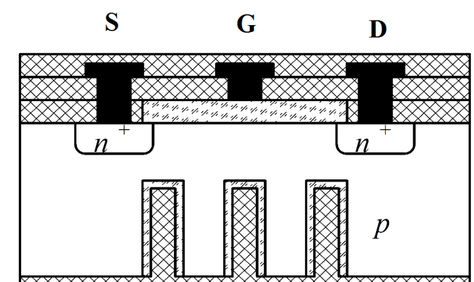

Fig. 11. Cross-section draft of MOSFET structure (operations of technological routing № 33 – 36).

Downloaded From: https://www.spiedigitallibrary.org/conference-proceedings-of-spie on 13 Nov 2021
Terms of Use: https://www.spiedigitallibrary.org/terms-of-use

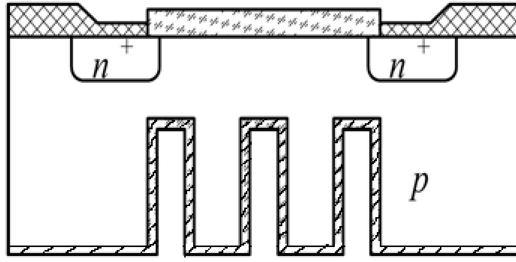

Fig. 7. Cross-section draft of MOSFET structure (operations of technological routing № 18 – 20)

4. OPERATIONS MODE CALCULATION AT MAKING OF N - CHANNEL MOS - PHOTOTRANSISTOR WITH BILATERAL ILLUMINATION OF CHANNEL AND SIMULATION OF IMPURITY DISTRIBUTION IN A STRUCTURE BY THE WAY OF TCAD MODELING ENVIRONMENT

4.1 Calculation of MOS - phototransistor with bilateral illumination of channel dimensions and determination the threshold tension a function of an impurity concentration on the semiconductor's surface

Calculation of dependence $U_{nop}(N_n)$ on the basis of analytical expressions allows to define the optimal value of concentration and type of an impurity on the semiconductor's surface, at that threshold tension corresponds to initial data of technological task. Calculation of dependence $U_{nop}(d_{ok})$ at an optimal value N_n gives an opportunity to define the sensitiveness of threshold tension to variations of gate oxide thickness. All dependences will allow to set forth requirements to the technological operations modes of route of MOS – phototransistor creation.

Will expect threshold tension of n - channel MOS - phototransistor at initial data: channel's length $L = 3 \cdot 10^{-6}\ m$; channel's width $z = 2 \cdot 10^{-6}\ m$; surface concentration of charge on the interface region $N_{ss} = 2 \cdot 10^{11} cm^{-2}$, concentration in p – substrate $N_p = 10^{15} cm^{-3}$, concentration of acceptor impurity $N_A = 1 \cdot 10^{24} m^{-3}$, concentration of donor impurity $N_D = 3 \cdot 10^{21} m^{-3}$, mobility of transmitters $\mu_n = 0.14\, m^2 / V \cdot s$, diffusive length of electron $L_n = 1.84 \cdot 10^{-4} m$, absorptance of optical radiation $\alpha = 6 \cdot 10^{-6} m^{-1}$, concentration of impurities in a gate $N_g = 10^{24} cm^{-3}$, time of life of unbasic charge transmitters $\tau_n = 1 \cdot 10^{-5} s$, relative dielectric constant of semiconductor (Si) $\varepsilon_S = 12$, relative inductivity of dielectric (SiO_2) $\varepsilon_d = 4$, intrinsic density of transmitters $n_i = 1.6 \cdot 10^{16} m^{-3}$, the radiated dose of alloying impurity $D_s = 0.05 \cdot 10^{-6} C \cdot cm^2$, the applied voltage $U_n = 5V$, $T = 300K$.

Will expect the thickness of substrate between the slot's bottom and gate's dielectric [11] d:

$$d = \frac{1}{\alpha} = \frac{1}{6 \cdot 10^6} = 0.16 \cdot 10^{-6}\ m \tag{1}$$

The area of channel S:

$$S = L \cdot z = 3 \cdot 10^{-6} \cdot 2 \cdot 10^{-6} = 6 \cdot 10^{-12}\ m^2 \tag{2}$$

Will find sectional area of slots A when $n = 5$ (3 slots and 5 spaces):

$$A = \frac{S}{n} = \frac{6 \cdot 10^{-12}}{5} = 1.2 \cdot 10^{-12}\ m^2 \tag{3}$$

Then length to the slot a equals:

$$a = \frac{A}{b} = \frac{1.2 \cdot 10^{-12}}{2 \cdot 10^{-6}} = 0.6 \cdot 10^{-6}\ m \tag{4}$$

Will expect the specific-capacitance of gate oxide:

$$C_{ox} = \frac{\varepsilon_0 \varepsilon_{ox}}{d} = \frac{8.85 \cdot 10^{-14} \cdot 3.6}{0.16 \cdot 10^{-6}} = 1.991 \cdot 10^{-6} F / cm^2 \ , \tag{5}$$

where ε_0 – dielectric constant of medium, and ε_{0x} – dielectric constant of oxide.

Downloaded From: https://www.spiedigitallibrary.org/conference-proceedings-of-spie on 13 Nov 2021
Terms of Use: https://www.spiedigitallibrary.org/terms-of-use

When intrinsic density of transmitters $n_i = 1.6 \cdot 10^{10} см^{-3}$ and $T = 300K$, Fermi level equals [16]:

$$\phi_F = \frac{k \cdot T \cdot \ln\left(N_p / n_i\right)}{q} = \frac{1.38 \cdot 10^{-23} \cdot 300 \cdot \ln\left(10^{15} / 1.6 \cdot 10^{10}\right)}{1.602 \cdot 10^{-19}} = 0.285\,V \quad (6)$$

Difference of works function provided that a gate and substrate are alloyed by the impurities with different conductivity type:

$$\phi_m = \frac{k \cdot T \cdot \left(\ln\left(\frac{N_A}{n_i}\right) + \ln\left(\frac{N_D}{n_i}\right)\right)}{q} = \frac{1.38 \cdot 10^{-23} \cdot 300 \cdot \left(\ln\left(\frac{10^{24}}{1.6 \cdot 10^{10}}\right) + \ln\left(\frac{10^{15}}{1.6 \cdot 10^{10}}\right)\right)}{1.602 \cdot 10^{-19}} = 1.106\,V \quad (7)$$

Will define the change of threshold voltage due to suballoying of substrate in area of channel [18]:

$$U_{thr} = \frac{D_s}{C_{ox}} = \frac{0.05 \cdot 10^{-6}}{1.991 \cdot 10^{-8}} = 0.285\,V \quad (8)$$

Thus threshold voltage equals:

$$U_{thr} = \phi_m - \frac{q \cdot N_{ss}}{C_{ox}} + \frac{D_s}{C_{ox}} + 2 \cdot \phi_F + \frac{\sqrt{2 \cdot q \cdot \varepsilon\varepsilon_{ox} \cdot N_p}}{C_{ox}} = 1.691\,V \quad (9)$$

Will expect dependences of threshold tension on the concentration of impurity on the surface of semiconductor. Figure 12 shows dependence $U_{пор}(N_p)$

Figure 12 shows that optimal value of impurity concentration in substrate is $N_p = 2 \cdot 10^{15} см^{-3}$, a type of impurity is acceptors (phosphorus). Thus threshold tension need to be adjusted by suballoying of substrate surface by acceptors (phosphorus) to the value of concentration $N_p = 2 \cdot 10^{15} см^{-3}$ on a depth, that approximately equal to the depth of bedding of drain-source.

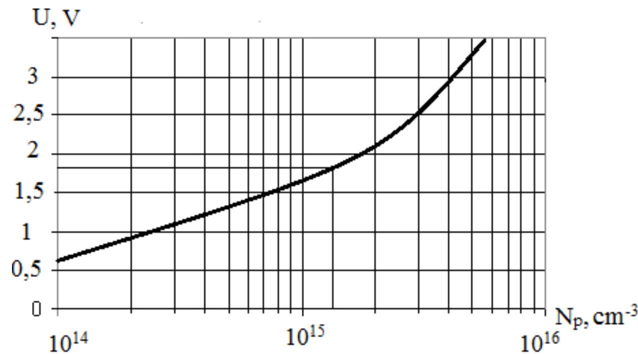

Fig. 12. Dependences of phototransistor's threshold tension on the concentration of impurity in substrate

Will expect dependence of threshold tension on the thickness of gate oxide. The dependence of phototransistor's threshold tension on the thickness of gate oxide $U_{пор}(d_{ок})$ is calculated with using of optimal value of impurity concentration in substrate. This dependence is represented on the figure 13.

Downloaded From: https://www.spiedigitallibrary.org/conference-proceedings-of-spie on 13 Nov 2021
Terms of Use: https://www.spiedigitallibrary.org/terms-of-use

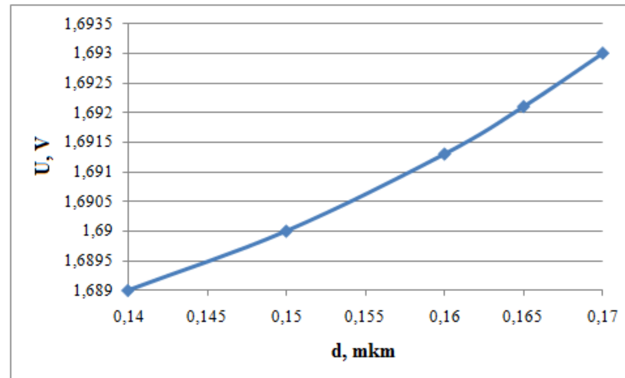

Fig. 13. Dependences of n-MOS-phototransistor's threshold tension on the thickness of gate oxide

4.2 Calculation of ionic implantation for creation of n channel - MOS - phototransistor with bilateral illumination of channel

Will define ions energy and irradiation dose, that are necessary for creation of area n^+-drain/source on a depth $x_{ds} = 0.3\, mkm$ by means of phosphorus implantation in p-type silicon and with concentration $C_B = 10^{16}\, cm^{-3}$ to provide concentration $C_{max} = 10^{19}\, cm^{-3}$.

Occurrence depth of area a n^+ -drain/source [14]:

$$x_{ds} = R_p + \Delta R_p \sqrt{2 \cdot ln\left(C_{max} / C_B\right)} \cdot \tag{10}$$

According to Eq (10):

$$x_{ds} = R_p + \Delta R_p \sqrt{4,6 \cdot lg \frac{5 \cdot 10^{19}}{1 \cdot 10^{16}}} = R_p + 4.12 \Delta R_p \cdot \tag{11}$$

Will plot dependence $R_p + 4.12\Delta R_p$ on energy in the range of 80 - 160 keV, using table's data 2 (Fig.14).

Table 2 – Value of normal mean paths and standard deviations of paths for the row of ions [14]

E, keV	11_B^+	27_{Al}^+	31_P^+	31_{As}^+	121_{Sb}^+
20 R_p	78	29	26	16	14
ΔR_p	32	11	9.4	3.7	2.4
40 R_p	161	56	49	27	23
ΔR_p	52	19	16.4	6.2	3.8
60 R_p	244	85	73	38	31
ΔR_p	71	27	23	8.4	5.1
80 R_p	324	114	98	48	38
ΔR_p	84	35	30	10.5	6.3
100 R_p	398	144	123	58	46
ΔR_p	94	42	35	12.5	7.4
120 R_p	469	175	149	68	53
ΔR_p	102	48	41	14.5	8.4
140 R_p	537	205	175	79	60
ΔR_p	110	54	47	16	9.5
160 R_p	603	236	201	89	67
ΔR_p	116	60	52	18	10.5
180 R_p	665	266	228	99	74
ΔR_p	121	60	57	20	11.5
200 R_p	725	297	254	110	81
ΔR_p	126	70	61	22	12.5

Downloaded From: https://www.spiedigitallibrary.org/conference-proceedings-of-spie on 13 Nov 2021
Terms of Use: https://www.spiedigitallibrary.org/terms-of-use

Will draw a line $x_{ds} = 0.3\ mkm$ on the fig. 14 and on an intersection will define $E = 122\ keV$.

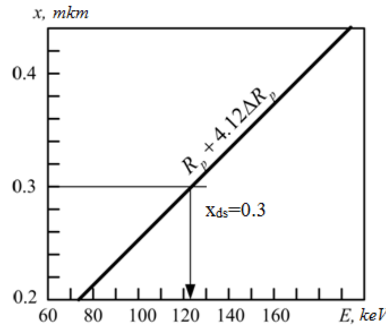

Fig. 14. Determination of ions energy.

For practical aims more comfortable to set energy of ions, that will be multiple 5 or 10 keV. Accept $E = 120\ keV$. Doing data interpolation (table 2), we will determine that for $E = 120\ keV$ $R_p = 149\ nm$, $\Delta R_p = 41\ nm$.

Will determine the irradiation dose [14]:

$$N = 2.5 \cdot \Delta R_p \cdot C_{max} = 2.5 \cdot 4.1 \cdot 10^{-6} \cdot 5 \cdot 10^{19} = 4.75 \cdot 10^{14}\ cm^{-2}. \quad (12)$$

A calculation of the implantation mode for creation of transistor structure.

Will write down equation for the occurrence depth of area a n^+-drain/source:

$$x_{ds} = R_{pa} + \Delta R_{pa}\sqrt{4.61 \cdot lg\left(C_{max} / C_B\right)} = R_{pa} + \Delta R_{pa}\sqrt{4.61 \cdot lg\left[3 \cdot 10^{18} / \left(2 \cdot 10^{16}\right)\right]} = R_{pa} + 3.16\Delta R_{pa} \quad (13)$$

For ions with the masses $M_1 > M_2$ in the range of energies of 20 – 100 keV the ratio between the path and standard deviation of path becomes [14]:

$$\Delta R_p / R_p \approx \gamma / 3, \quad (14)$$

or

$$\Delta R_p = \gamma R_p / 3. \quad (15)$$

Thus

$$x_{ds} = R_{pa} + 3.12 \cdot \gamma R_{pa} / 3 \approx 2R_p, \quad (16)$$

where

$$R_{pa} = x_{ds} / 2 = 0.3 / 2 = 0.15\ mkm. \quad (17)$$

Using table 2, accept $E_a = 140\ keV$, than $R_{pa} = 0{,}175\ mkm$, $\Delta R_{pa} = 0{,}047\ mkm$. Thus:

$$x_{ds} = 0.175 + 3.12 \cdot 0.047 = 0.326\ mkm. \quad (18)$$

A difference with a necessary value does not exceed 10%, that possibly.

Irradiation dose of phosphorus ions [14]:

$$N_a = \sqrt{2\pi} \cdot \Delta R_{pa} \cdot C_{max} = \sqrt{2 \cdot 3.14} \cdot 5.38 \cdot 10^{-6} \cdot 3 \cdot 10^{18} = 4 \cdot 10^{13}\ cm^{-2}. \quad (19)$$

4.3 Calculation of impurity distribution for two-stage diffusion at forming of area n^+-drain/source

Will expect impurity distribution for two-stage diffusion of phosphorus in silicon, that is realized under existing conditions: $T_1 = 1250^o C$, $t_1 = 10$ min, $T_2 = 1150^o C$, $t_2 = 2\ hours$. Will define the occurrence depth of p - n junction.

First of all will define the diffusion coefficients of phosphorus in silicon by fig. 15 [14]: $D_1 = 4 \cdot 10^{-12} cm^2 / s$, $D_2 = 4 \cdot 10^{-13} cm^2 / s$.

Since:

$$D_1 t_1 = 4 \cdot 10^{-12} \cdot 10 \cdot 60 = 2.4 \cdot 10^{-9} \approx D_2 t_2 = 4 \cdot 10^{-13} \cdot 2 \cdot 60 \cdot 60 = 2.88 \cdot 10^{-9} cm^2, \quad (20)$$

Will define tabular parameters α i z: [10]

$$\alpha = \sqrt{D_1 t_1 / (D_2 t_2)} = \sqrt{2.4 \cdot 10^{-9} / (2.88 \cdot 10^{-9})} \approx 0.9, \quad (21)$$

$$z = \frac{x^2}{4(D_1 t_1 + D_2 t_2)} = \frac{x^2}{4 \cdot (2.4 \cdot 10^{-6} + 2.88 \cdot 10^{-9}} = \frac{x^2}{2.11 \cdot 10^{-8}}. \quad (22)$$

Downloaded From: https://www.spiedigitallibrary.org/conference-proceedings-of-spie on 13 Nov 2021
Terms of Use: https://www.spiedigitallibrary.org/terms-of-use

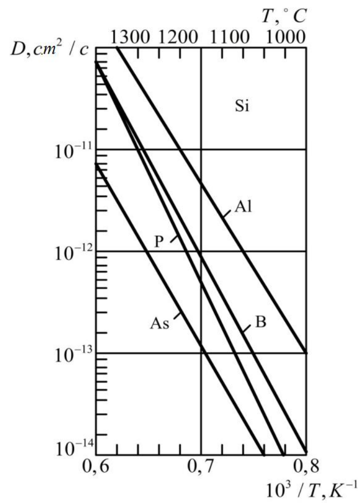

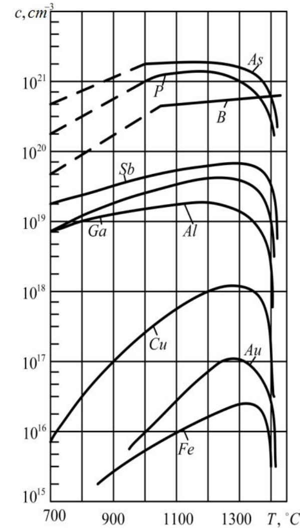

Fig. 15. Dependences of the impurity diffusion coefficients in silicon on the temperature [14]

Fig. 16. Dependences of maximum solubility of impurity elements in silicon on the temperature [14]

Will define a superficial concentration after dopant up-diffusion. According to dependences $C = f(T)$ (fig. 16) under existing conditions $T_1 = 1250^o C$ the concentration $C_{01} = 1.2 \cdot 10^{21} cm^{-3}$.

The superficial concentration after dopant up-diffusion [14]:

$$C_{02} = \frac{2C_{01}}{\pi} arctg\alpha = \frac{2 \cdot 1.2 \cdot 10^{21}}{3.14} arctg 0.9 = 5.6 \cdot 10^{20} cm^{-3} \tag{23}$$

Using table's data will set a value $z = 0.1, 0.3, 0.5$ etc and will define for $\alpha = 0.9$ the value of integral. Before making a graph we will find a depth (cm):

$$x = 2\sqrt{(D_1 t_1 + D_2 t_2) \cdot z} = 1.45 \cdot 10^{-4} \sqrt{z}. \tag{24}$$

On the predeposition diffusion stage impurity distribution equals [14]:

$$C(x) = 1.2 \cdot 10^{21} erfc \frac{x}{2\sqrt{2.4 \cdot 10^{-9}}} = 1.2 \cdot 10^{21} erfc \frac{x}{0.98 \cdot 10^{-4}}. \tag{25}$$

Both profiles (after predeposition diffusion 1 and after dopant up-diffusion 2) are shown on fig. 17. On the predeposition diffusion stage the diffusion depth folds approximately $3/4$ of complete depth after dopant up-diffusion.

The occurrence depth of p-n junction- will define by approximate formula [14]:

$$x_j \approx 6\sqrt{Dt} \cdot \tag{26}$$

Will take into account the presence of two stages compared by the depth of diffusion:

$$x_j \approx 6\sqrt{D_1 t_1 + D_2 t_2} = 6\sqrt{5.28 \cdot 10^{-9}} = 4.35 \cdot 10^{-4} cм = 4.35\ mkm. \tag{27}$$

For comparison will build the profile of distribution without the account of the real relationship between the $D_1 t_1$ and $D_2 t_2$, using Gaussian curve when $(Dt)_{ef} = D_1 t_1 + D_2 t_2$:

$$C(x) = \frac{N}{\sqrt{\pi (Dt)_{ef}}} \exp\left(-\frac{x^2}{4(Dt)_{ef}}\right), \tag{28}$$

where

$$N = 2C_{01}\sqrt{\frac{D_1 t_1}{\pi}} = 2 \cdot 1.2 \cdot 10^{21} \sqrt{\frac{2.4 \cdot 10^{-9}}{3.14}} = 6.6 \cdot 10^{16} cm^{-2}, \tag{29}$$

Will find:

$$C(x) = \frac{6.6 \cdot 10^{16}}{\sqrt{3.14 \cdot 5.28 \cdot 10^{-9}}} \exp\left(-\frac{x^2}{2.11 \cdot 10^{-8}}\right) = 5.1 \cdot 10^{23} \exp\left(-\frac{x^2}{2.11 \cdot 10^{-8}}\right). \tag{30}$$

Downloaded From: https://www.spiedigitallibrary.org/conference-proceedings-of-spie on 13 Nov 2021
Terms of Use: https://www.spiedigitallibrary.org/terms-of-use

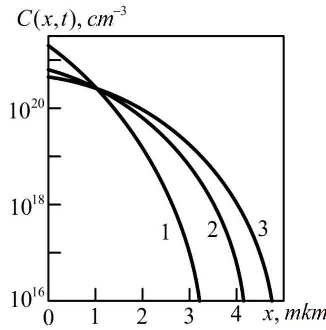

Fig. 17. Calculation profiles of phosphorus distribution at two-stage diffusion

This distribution is shown on fig. 17 by a curve 3, that well approximates a curve 2 on small depths, but at $x \geq 4\ \mu m$ sets too high a concentration almost on an order.

4.4 Modeling of impurity distribution and structure of MOS- phototransistor with bilateral illumination of channel in the system of device and technology simulation TCAD

Will model impurity distribution in structure of MOS- phototransistor with bilateral illumination of channel in the system of TCAD. For this purpose it is necessary to start subprogram Deckbuild.

After that it it is necessary to open the program with expansion (*.in) by pressure of icon "Open", that is written for this modeling and to press on the key of "Run". On the lower half of screen there will be a process of account for the further construction of image by means of subprogram Tonyplot (for a two-dimensional design).

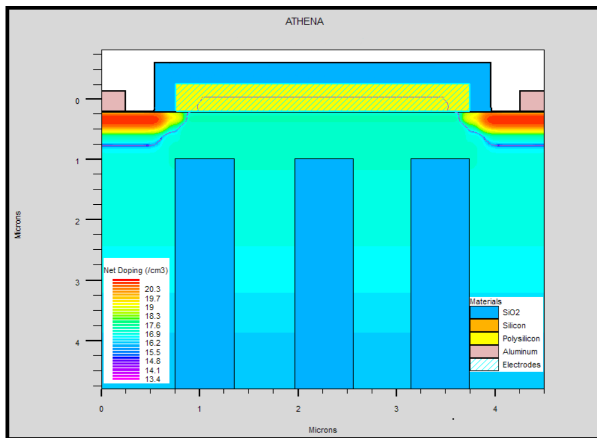

Fig. 18. Resulting impurity distribution in the phototransistor in subprogram Tonyplot

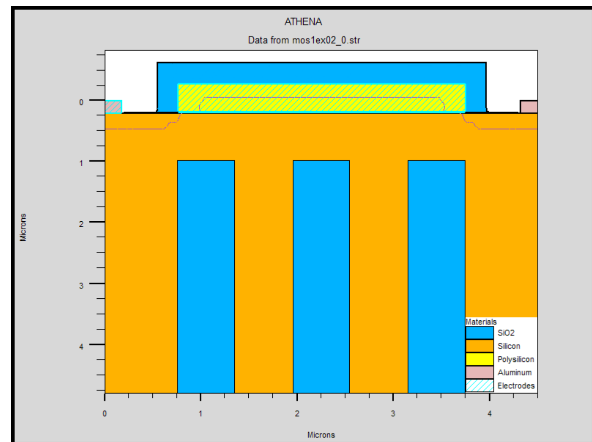

Fig. 19. Modeling of MOS - phototransistor structure

As a result of technological process modeling of MOS - phototransistor with bilateral illumination of channel creation we get resulting impurity distribution (fig. 18), where the corresponding arsenic (As) impurity concentrations mark colors. Figure 18 shows, that a most impurity concentration (red area) is in area of source and drain under the layer of metal, id est a concentration $N = 20.3\ см^{-3}$ is on the depth of 0.5 mkm of source and drain area.

After impurity distribution modeling in the structure of MOS - phototransistor with bilateral illumination of channel we have the modeling of phototransistor structure (fig. 19) and graphing of dependence of phototransistor source current on gate tension (fig. 20)

Figure 20 shows, that gate tension varies from 0 V to 0.5 V and the source current doesn't change. But at the further increase of tension from 0.5 V to 3 V, a current begins to increase.

Downloaded From: https://www.spiedigitallibrary.org/conference-proceedings-of-spie on 13 Nov 2021
Terms of Use: https://www.spiedigitallibrary.org/terms-of-use

Complete technological route of n - channel MOS - phototransistor with bilateral illumination of channel making includes adjustment of calculated threshold tension $U_{por} = 1.8\,V$, by the ionic doping to the value $N_p = 2 \cdot 10^{15}\,cm^{-3}$ in obedience to the calculated transistor sizes: substrate thickness between a slot bottom and the gate dielectric $d = 0.16 \cdot 10^{-6}\,m$, area of channel $S = 6 \cdot 10^{-12}\,m^2$, sectional area of slots $A = 1.2 \cdot 10^{-12}\,m^2$ at $n = 5$, length of the slot $a = 0.6 \cdot 10^{-6}\,m$.

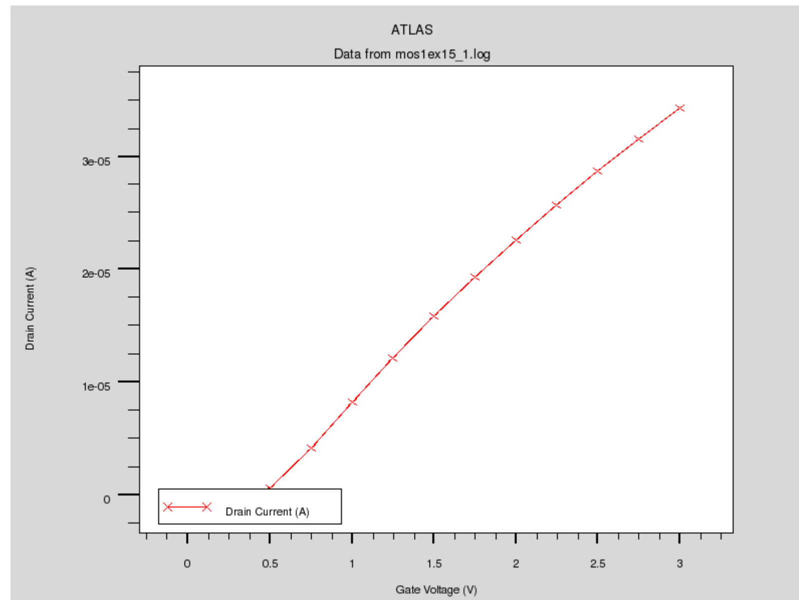

Fig. 20. Dependences of phototransistor drain current on gate tension

5. DETERMINATION OF CONVERSION FUNCTION AND SENSITIVENESS EQUATION OF OPTICAL CONVERTOR ON THE BASIS OF MOSFET WITH BILATERAL ILLUMINATION OF CHANNEL

For a further sensitivity to measuring of optical power a device the electric chart of that is shown on fig. 21 is offered. A device on the basis of optical transducer contains BPT and MOSFET with bilateral illumination of channel that is a photosensitive element. On collector-drain electrodes of the offered structure exists negative resistance that corresponds to falling section on current-voltage characteristic. A photosensitive device feeds from the source of permanent tension U_1 (supply voltage) and U_2 (control voltage)

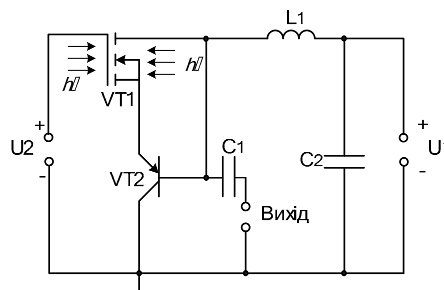

Fig. 21. Electric chart of device on the basis of bipolar and MOSFET with bilateral illumination of channel

For determination of basic parameters that characterize work of device on the basis of optical transformer (fig. 21), it is necessary to count an impedance on electrodes drain-collector of transistors VT1 and VT2 according to the equivalent chart of device for an alternating current (fig. 22). For realization of calculations chart on fig. 22 is regenerated in more comfortable (fig. 23).

Downloaded From: https://www.spiedigitallibrary.org/conference-proceedings-of-spie on 13 Nov 2021
Terms of Use: https://www.spiedigitallibrary.org/terms-of-use

In an equivalent chart on fig. 23 next denotations are used:

$$Z_1 = R'_ç + j\omega L_ç;\ Z_2 = \frac{R_{çâ}}{1+\omega^2 R_{çâ}^2 C_{çâ}^2} - j\frac{\omega R_{çâ}^2 C_{çâ}}{1+\omega^2 R_{çâ}^2 C_{çâ}^2};\ Z_3 = -j/(\omega C_{çñ});\ Z_6 = R'_c + j\omega L_c;\ Z_7 = j\omega L_1;\ Z_9 = R'_â + j\omega L_â;\ Z_{11} = R_á;$$

$$Z_4 = \frac{R_{câ}}{1+\omega^2 R_{câ}^2 C_{câ}^2} - j\frac{\omega R_{câ}^2 C_{câ}}{1+\omega^2 R_{câ}^2 C_{câ}^2};\ Z_5 = \frac{R_c}{1+\omega^2 R_c^2 C_c^2} - j\frac{\omega R_c^2 C_c}{1+\omega^2 R_c^2 C_c^2};\ Z_8 = \frac{R_{\hat{a}}}{1+\omega^2 R_â^2 C_â^2} - j\frac{\omega R_â^2 C_â}{1+\omega^2 R_â^2 C_â^2};\quad Z_{10} = R'_á + j\omega L_á;$$

$$Z_{12} = \frac{R_ê}{1+\omega^2 R_ê^2 C_ê^2} - j\frac{\omega R_ê^2 C_ê}{1+\omega^2 R_ê^2 C_ê^2};\ Z_{13} = R'_ê + j\omega L_ê;\ Z_{15} = R'_e + j\omega L_e;\ \alpha = \alpha_1 - j\alpha_2;\ Z_{14} = \frac{R_e}{1+\omega^2 R_e^2 C_e^2} - j\frac{\omega R_e^2 C_e}{1+\omega^2 R_e^2 C_e^2}.$$

For conversion function determination it is necessary to find dependence of generation frequency on the value of optical radiation power. The system of Kirchhoff equations, made on the basis of equivalent chart (fig. 23), is described by expression (31).

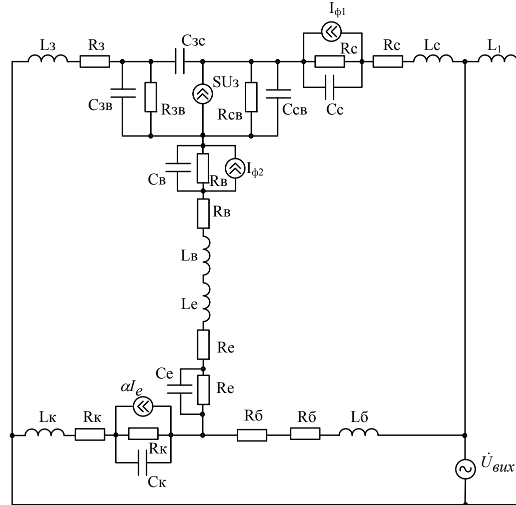

Fig. 22. Equivalent chart of device on the basis of MOSFET with bilateral illumination of channel for an alternating current

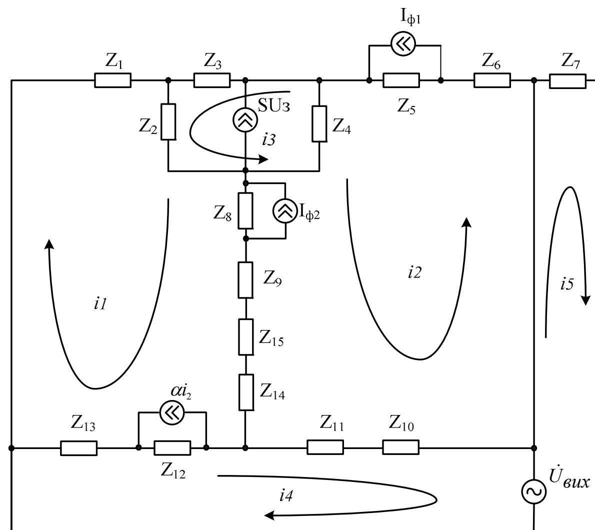

Fig. 23. Converted equivalent chart of device on the basis of MOSFET with bilateral illumination of channel

Downloaded From: https://www.spiedigitallibrary.org/conference-proceedings-of-spie on 13 Nov 2021
Terms of Use: https://www.spiedigitallibrary.org/terms-of-use

$$
\begin{cases}
\dot{U}_{вих} = Z_7 i_5, \\
\dot{U}_{вих} = (Z_{13} + Z_{12} + Z_{11} + Z_{10}) i_4 + Z_{12} \alpha i_2 - (Z_{13} + Z_{12}) i_1 + (Z_{10} + Z_{11}) i_2, \\
0 = (Z_4 + Z_8 + Z_9 + Z_{15} + Z_{14} + Z_{11} + Z_{10} + Z_6 + Z_5) i_2 + Z_8 I_{ф2} + \\
+(Z_8 + Z_9 + Z_{14} + Z_{15}) i_1 + (Z_{10} + Z_{11}) i_4 + Z_4 SU_з - Z_4 i_3 - Z_5 I_{ф1}, \\
0 = (Z_1 + Z_2 + Z_8 + Z_9 + Z_{15} + Z_{14} + Z_{12} + Z_{13}) i_1 + Z_2 i_3 + Z_2 SU_з + Z_8 I_{ф2} + \\
(Z_8 + Z_9 + Z_{15} + Z_{14}) i_2 - Z_{12} \alpha i_2 - (Z_{12} + Z_{13}) i_4, \\
0 = (Z_3 + Z_2 + Z_4) i_3 + Z_2 i_1 + (Z_3 + Z_2 - Z_4) SU_з - Z_4 i_2,
\end{cases}
\tag{31}
$$

Conversion function of device measuring channel on the basis of bipolar and MOSFET with bilateral illumination described by expression (32), and sensitiveness of device measuring channel - by expression (33):

$$
F = \frac{1}{2\pi} \sqrt{\frac{R_c^2(P) C_c(P)\left(C_{зс} + C_c(P)\right) - L_1 C_{зс} + \sqrt{A_2^2 + 4A_1}}{2A_1}}; \tag{32}
$$

$$
\begin{aligned}
S_P^F = \frac{\sqrt{2}}{8} \Bigg[\Bigg\{ & 2A_3 \left(\frac{\partial}{\partial P} R_c(P) \right) + A_4 \left(\frac{\partial}{\partial P} C_c(P) \right) + R_c^2(P) C_c(P) \left(\frac{\partial}{\partial P} C_c(P) \right) + \frac{1}{2} \Bigg(2A_2 \Bigg(-2A_3 \left(\frac{\partial}{\partial P} R_c(P) \right) - A_4 \left(\frac{\partial}{\partial P} C_c(P) \right) - \\
& - -R_c^2(P) C_c(P) \left(\frac{\partial}{\partial P} C_c(P) \right) \Bigg) + 8A_1 R_c(P) \times \left(\frac{\partial}{\partial P} R_c(P) \right) + +8A_1 C_c(P) \left(\frac{\partial}{\partial P} C_c(P) \right) \Bigg) \Bigg/ \sqrt{A_2^2 + 4A_1} \Bigg\} \Bigg/ A_1 - \\
& - \frac{2\left(-A_2 + \sqrt{A_2^2 + 4A_1}\right)\left(\frac{\partial}{\partial P} R_c(P)\right)}{A_1 R_c(P)} - \frac{2\left(-A_2 + \sqrt{A_2^2 + 4A_1}\right)\left(\frac{\partial}{\partial P} C_c(P)\right)}{A_1 C_c(P)} \Bigg] \Bigg/ \left[\pi \sqrt{\frac{-A_2 + \sqrt{A_2^2 + 4A_1}}{A_1}} \right],
\end{aligned}
\tag{33}
$$

where

$$
A_1 = L_1 C_{зс} R_c^2(P) C_c^2(P);\ A_2 = L_1 C_{зс} - R_c^2(P) C_c(P)\left(C_{зс} + C_c(P)\right);\ A_3 = R_c(P) C_c(P)\left(C_{зс} + C_c(P)\right);
$$
$$
A_4 = R_c^2(P)\left(C_{зс} + C_c(P)\right).
$$

Figure 24 shows dependences of conversion function of device measuring channel and dependence of sensitiveness on the change of optical power.

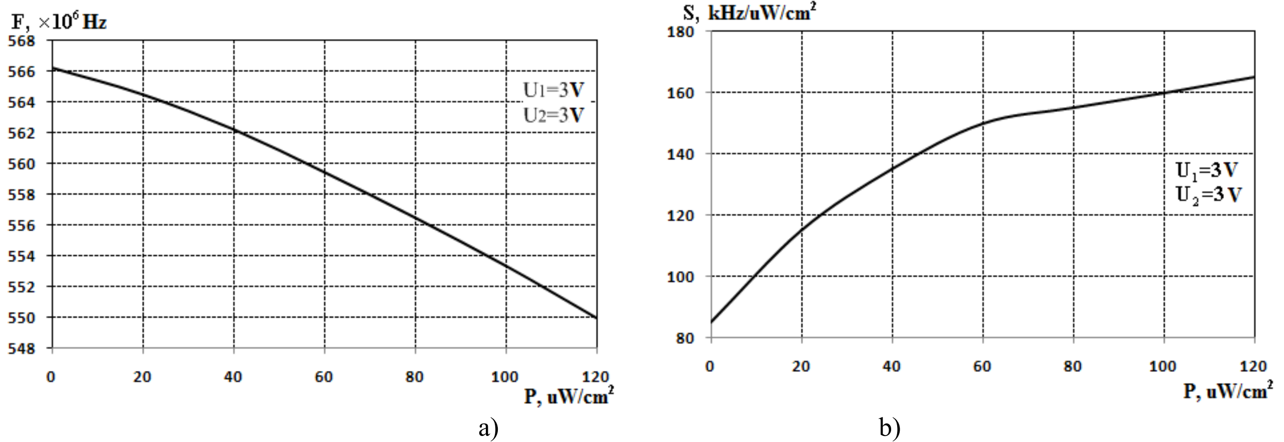

Fig. 24. Theoretical conversion function of device measuring channel (a) and dependence of sensitiveness of device measuring channel on the change of optical radiation power (b)

Figure 24 shows, that with the increase of optical power from 0 to 120 uW/cm^2 the generation frequency diminishes from 566.2 MHz to 550 MHz, thus supply voltage and control voltage have value of 3 V. Figure. 24 shows, that with the change of optical radiation power from 0 to 120 мкВт/см^2, sensitiveness changes from 85.2 to 165.1 kHz/uW/cm^2.

Downloaded From: https://www.spiedigitallibrary.org/conference-proceedings-of-spie on 13 Nov 2021
Terms of Use: https://www.spiedigitallibrary.org/terms-of-use

6. CONCLUSIONS

Radiomeasuring optical transducer on the basis of the bipolar and MOS transistors structure with negative resistance and has been proposed and investigated. A mathematical model of the radiomeasuring optical transducer has been developed. Complete technological route of n - channel MOS - phototransistor with bilateral illumination of channel making includes adjustment of calculated threshold tension $U_{por} = 1.8\,V$, by the ionic doping to the value $N_p = 2 \cdot 10^{15} cm^{-3}$ in obedience to the calculated transistor sizes: substrate thickness between a slot bottom and the gate dielectric $d = 0.16 \cdot 10^{-6}\ m$, area of channel $S = 6 \cdot 10^{-12}\ m^2$, sectional area of slots $A = 1.2 \cdot 10^{-12}\ m^2$ at $n = 5$, length of the slot $a = 0.6 \cdot 10^{-6}\ m$. With the increase of optical power from 0 to 120 мкВт/см^2 the generation frequency diminishes from 566,2 MHz to 550 MHz, thus supply voltage and control voltage have value of 3 V. Figure. 24 shows, that with the change of optical radiation power from 0 to 120 uW/cm^2, sensitiveness changes from 85.2 to 165.1 kHz/uW/cm^2.

Authors: *D. Sc., Professor Oleksandr V. Osadchuk, Vinnytsia National Technical University, 95 Khmelnytske shose, Vinnytsia, Ukraine, 21021, E-mail: osadchuk69@mail.ru; D. Sc., Professor Volodymyr S. Osadchuk, Vinnytsia National Technical University, 95 Khmelnytske shose, Vinnytsia, Ukraine, 21021, E-mail: osadchuk.vs38@gmail.com; Ph.D.* Olena M. Zhahlovska, *Vinnytsia National Technical University, 95 Khmelnytske shose, Vinnytsia, Ukraine, 21021, E-mail: osadchuk.vs38@gmail.com; Ph.D*

REFERENCES

[1] Schaumburg H., [Sensoren], Stuttgart, Teubner, (1992).
[2] Hotra Z.Yu., [Microelectronic sensors of physical quantities. Edited In 3 volumes], Lvov, League-Press (2003).
[3] Novitsky P.V., Knoring V.G., Gutnikov V.S., [Digital devices with frequency sensors], Leningrad, Energy (1970).
[4] Zabolotna N.I., Pavlov S.V., Radchenko K.O. Stasenko V.A., Wójcik W., Kussambayeva N., "Diagnostic efficiency of Mueller-matrix polarization reconstruction system of the phase structure of liver tissue," Proc. SPIE 9816, Optical Fibers and Their Applications 2015, 98161E (2015).
[5] Kholin V.V., Chepurna O.M, Shton I.O., Voytsehovich V.S., Azarov O.D., Pavlov S.V., Gamaleia N.F., Harasim D., "Methods and fiber optics spectrometry system for control of photosensitizer in tissue during photodynamic therapy," Proc. SPIE 10031, Photonics Applications in Astronomy, Communications, Industry, and High-Energy Physics Experiments 2016, 1003138 (2016).
[6] Osadchuk V.S., Osadchuk A.V. "Radiomeasuring Microelectronic Transducers of Physical Quantities," Proceedings of the 2015 International Siberian Conference on Control and Communications (SIBCON), (2015).
[7] Osadchuk O., Osadchuk V., Osadchuk I., Kolimoldayev M., Komada P., Mussabekov K., "Optical transducers with frequency output," Proc. SPIE 10445, Photonics Applications in Astronomy, Communications, Industry, and High Energy Physics Experiments 2017, 104451X (2017).
[8] Osadchuk O., Osadchuk I., Suleimenov B., Zyska T., Arman A., Tleshova A., Grądz Ż., "Frequency pressure transducer with a sensitivity of mem capacitor on the basis of transistor structure with negative resistance," Proceedings of SPIE 10445, (2017).
[9] Zuev V., "Photoelectric MDS-devices," Radio and communication (1983).
[10] Kostenko V.L., [Measuring convertors on the basis of combine solid-state structures], Shvec E.Ya., Kyselov E.N., Omelchuk N.A., Zaporozhie, publishers (2001).
[11] Osadchuk V., Osadchuk O., Ilchenko O., "Transistors Photo Sensitive Sensor with Two-Way Channel Lighting," Applicant and patent holder Vinnitsa National Technical University. - №200900890; Bull. N.12 (2009).
[12] Chernyaev V.N., [Technology of production of integrated microcircuits and microprocessors], Radio and Communication (1987).
[13] Rosado L., [Physical Electronics and Microelectronics], Higher School (1991).
[14] Kurnosov A.I., [Technology of production of semiconductor devices and integrated microcircuits: Proc. A manual for universities on spec. "Semiconductors and dielectrics"], Higher Education (1986).
[15] Zykov D.D., [Systems for automated modeling and design of technological processes and technological routes for the production of microwave MIS, production optimization (the basis of CAD Synopsys TCAD)], Tomsk, TUSUR (2010).

Downloaded From: https://www.spiedigitallibrary.org/conference-proceedings-of-spie on 13 Nov 2021
Terms of Use: https://www.spiedigitallibrary.org/terms-of-use

[16] Azarov O., Chernyak O., Komada P., Kozhambardiyeva M., Kalizhanova A., "High-speed counters in Fibonacci numerical system," Proc. SPIE 10445, Photonics Applications in Astronomy, Communications, Industry, and High Energy Physics Experiments 2017, 1044522 (2017).
[17] Azarov O., Troianovska T.I., Savytska L.A., Savchuk T.O., Nykyforova L.E., Otryshko V.A., Suleimenov B., Gromaszek K., Kozbekova A., Sagymbekova A., "Quality of content delivery in computer specialists training system," Proc. SPIE 10445, Photonics Applications in Astronomy, Communications, Industry, and High Energy Physics Experiments (2017).
[18] Azarov O.D., Krupelnitskyi L.V. and Komada P., "AD systems for processing of low frequency signals based on self calibrate ADC and DAC with weight redundancy," Przeglad Elektrotechniczny 93(5), 125-128 (2017).
[19] Azarov O.D., Dudnyk O.D., Duk M., Porubov D., "Static and dynamic characteristics of the self-calibrating multibit ADC analog components," Proc. SPIE 8698, Optical Fibers and Their Applications 2012, 86980N (2013).
[20] Azarov A.D., Chernyak A.I., Chernyak P.A., "Class of numerical systems for pipeline bit sequential development of multiple optoelectronic data streams," Proc. SPIE 4425, Selected Papers from the International Conference on Optoelectronic Information Technologies, (2001).
[21] Gotra Z., Golyaka R., Pavlov S. and Kulenko S., "High resolution differential thermometer," Technology and Design in Electronic Apparatuses 6, 19-23 (2009).

Downloaded From: https://www.spiedigitallibrary.org/conference-proceedings-of-spie on 13 Nov 2021
Terms of Use: https://www.spiedigitallibrary.org/terms-of-use